DOI: 10.15413/ajcec.2017.0253, 5(12): 000-000, December 2017
ISSN 2315-7712

Research Paper

Non-linear analysis of bending GFRP tube concrete member

Accepted 12th December, 2017

Jiaxiang Wang, Zhigang Song and Cheng Fan*

Research Center for Numerical Tests on Material Failure, Dalian University, Dalian 116622, China.

*Corresponding author. E-mail: fancheng@dlu.edu.cn.

ABSTRACT

In order to study the factors that influence anti-bending mechanical properties of GFRP tube confined concrete beams and better applied to engineering, the influence of different thickness of GFRP tube, concrete strength grade, the section form and strength of steel were analyzed using finite element analysis software ABAQUS when the beam is in compression condition in this paper. The results showed that the bearing capacity of beams was improved by increasing the GFRP tube thickness, improving the core concrete strength and increasing steel area and strength. The numerical results were in good agreement with the experimental one. The anti-bending bearing capacity formula was in good agreement with the experimental results.

Keywords: GFRP tube, ABAQUS, mechanical property, the bearing capacity.

INTRODUCTION

The compression member's constraint effect of GFRP tube on the core concrete was better than that of the bending, but it was more common that the GFRP concrete composite components bear the bending moment in actual construction, such as large eccentric compression components and small eccentric compression members and tension-flexure components were not only to bear the axial force but also to bear the bending moment (Cao, 2013; Xia, 2011). Therefore, it is necessary to study the flexural properties of GFRP confined concrete members (Li, 2013; Zhang and Wang, 2014).

In this paper, the existing test results was simulated using the finite element software ABAQUS. Based on these facts the numerical results were in good agreement with the experimental one, the influence of different thickness of GFRP tube, concrete strength grade, the section form and strength of steel when the beam under the compression were analyzed.

FINITE ELEMENT BASIS

Concrete constitutive relation

By verifying a large number of numerical results, the constitutive relation of core concrete used the concrete constitutive relation model of Zhao et al. (2003) and the expression is given as:

$$\sigma_c = \begin{cases} \sigma_0\left[A\left(\frac{\varepsilon}{\varepsilon_0}\right) - B\left(\frac{\varepsilon}{\varepsilon_0}\right)^2\right] & (\varepsilon \le \varepsilon_0) \\ \sigma_0(1-q) + \sigma_0 q\left(\frac{\varepsilon}{\varepsilon_0}\right)^{0.1\theta'} & \theta \ge 1.12(\varepsilon \le \varepsilon_0) \\ \sigma_0 \frac{\varepsilon}{\varepsilon_0}\left[1/\beta\left(\frac{\varepsilon}{\varepsilon_0} - 1\right)^2 + \frac{\varepsilon}{\varepsilon_0}\right] & \theta \ge 1.12(\varepsilon \le \varepsilon_0) \end{cases} \quad (1)$$

The calculation of the relevant parameters is referred to (Zhao et al., 2003) the tensile stress relationship model of concrete given as:

$$\sigma_t = \begin{cases} (1.2x - 0.2x^6)\sigma_p & \varepsilon \le \varepsilon_p \\ \dfrac{x}{0.31\sigma_p(x-1)^{1.7} + x} & \varepsilon \le \varepsilon_p \end{cases} \quad (2)$$

Where σ_p means peak stress, $\sigma_p = 0.26(f_{cu})^{2/3}$, ε_p means peak strain, $\varepsilon_p = 43.1\sigma_p(\mu\varepsilon)$.

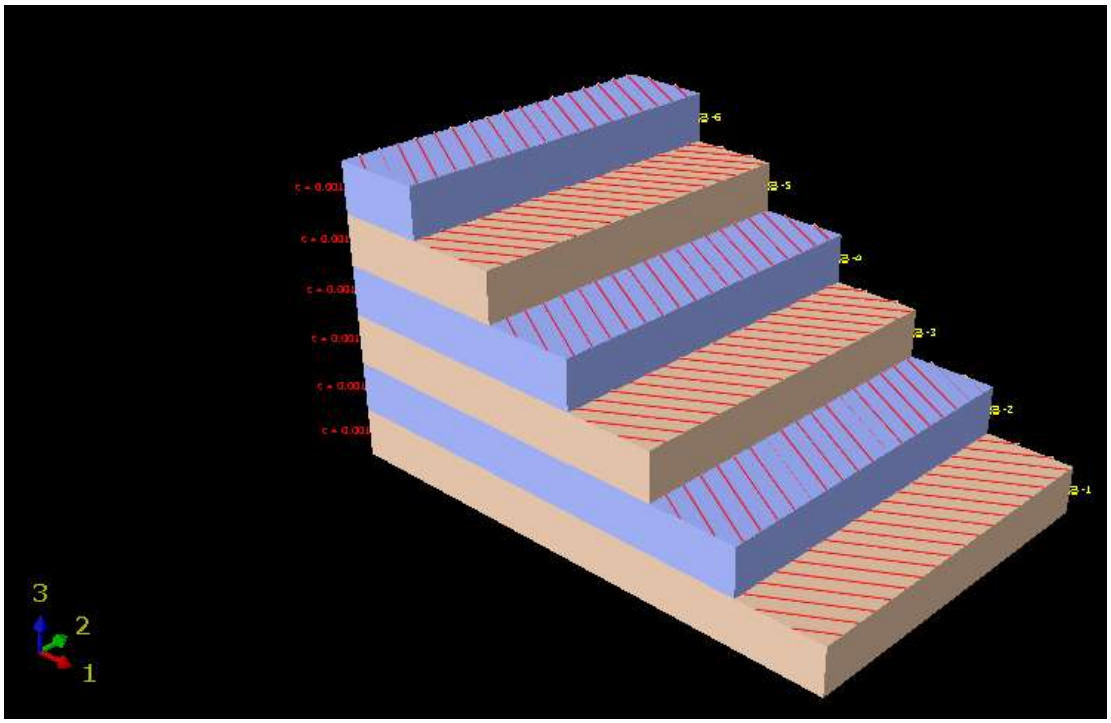

Figure 1: GFRP tube paving method.

Table 1: 6 mm GFRP tube paving situation.

Total thickness		Pavement design					
6 mm	Single layer angle	30	-30	30	-30	30	-30
	Single layer thickness	0.001	0.001	0.001	0.001	0.001	0.001

Constitutive model of GFRP tube

The mechanical properties of GFRP tube (Figure 1) on the elastic section was simulated using ABAQUS single-layer plate model and the Hashin failure criteria (Hashin, 1980) was used in ABAQUS to approximate and simulate the composite material's damage evolution process. The correlation parameter of single layer plate was calculated using the analytical method in the mesomechanics of the composite materials (Qin, 2010). Thereafter, a pavement design about GFRP tube was provided, for example, pavement design to 6 mm thick GFRP tube (Table 1).

Establishment the finite element model

In order to improve the efficiency of numerical calculation,1/2 model was calculated, applying the symmetrical constraint about Z axis on the mid-span, the concrete and the pad were using eight-node hexahedral reduction integral unit (C3D8R), while the steel and GFRP tubes were modeled using the shell element S4R (four-node reduction integral), in the thickness direction. Figure 2 shows the use of three integral points Poisson integral, the various parts of the finite element model and boundary conditions.

EXPERIMENTAL VERIFICATION

In order to verify the accuracy of the numerical model, the numerical simulation in the bearing capacity was compared with the experimental data in Qin et al. (2009) and deflection M- μ curve (Figure 3). In this paper, the detailed experimental data and the bearing capacity calculated was compared with the experimental data in Table 2.

Table 2 and Figure 3 shows the numerical simulation was in good agreement with the experimental data and the calculation curve were under the experimental curve; the calculation was safe and the model accuracy verified.

Analysis of influencing factors of M-μ curve

The factors affecting the component's bending properties were the fiber winding angle of the GFRP tube, the wall

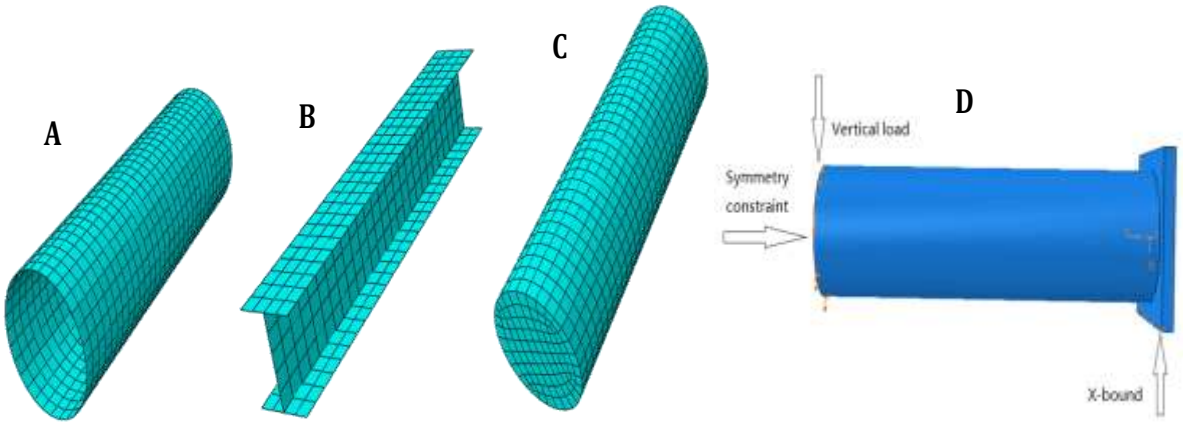

Figure 2: Each part of the component model boundary and the meshing a) GFRP tube; b) Steel bone; c) Concrete and d) Boundary and load conditions.

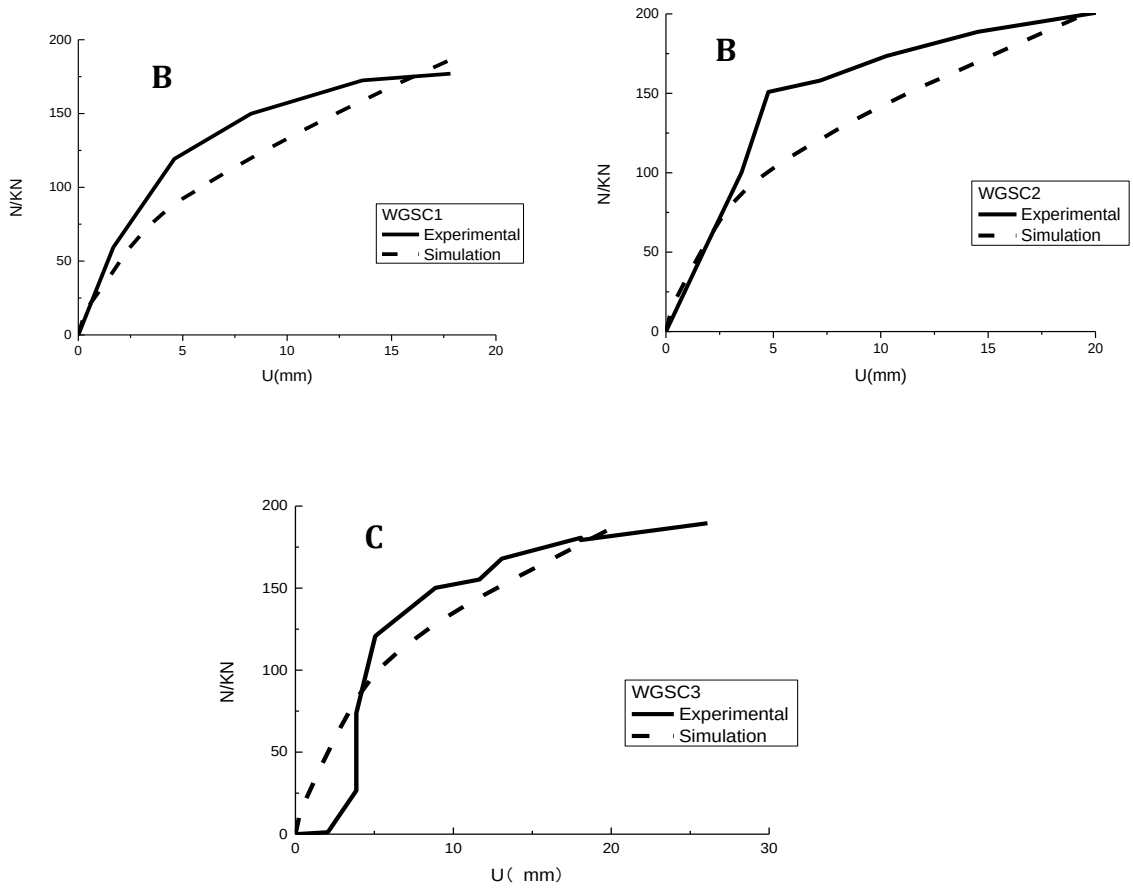

Figure 3: Experimental curve compared with simulation curve. a) WGSC1; b) WGSC2 and c) WGSC3.

Table 2: Detailed data.

Specimen number	t	L(mm)	D(mm)	F_c(MPa)	Fiber winding angle	N_{exp}	N_{cal}	N_{exp}/N_{cal}
WGSC1	5	1200	200	48.6	80	177	187	0.95
WGSC2	5	1200	200	48.6	60	201	202	0.99
WGSC3	3	1200	200	48.6	60	185	186	0.99

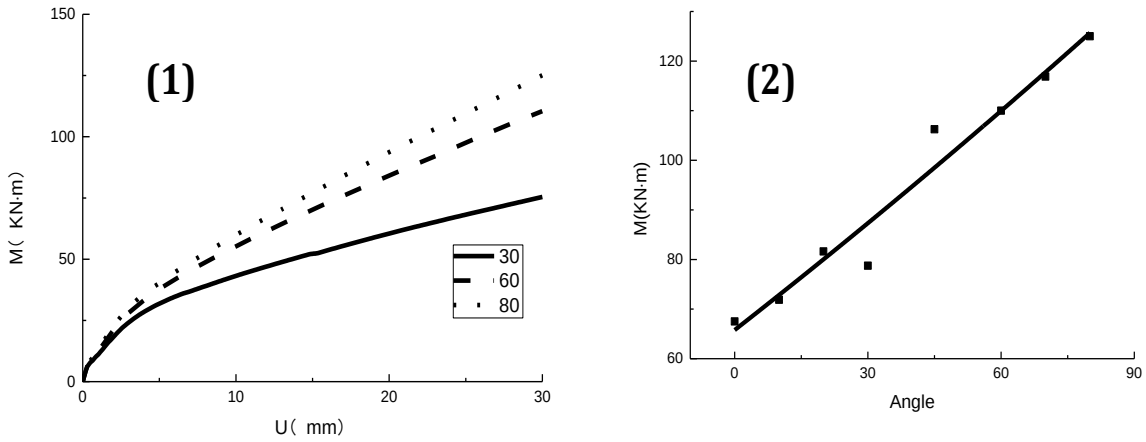

Figure 4a: Numerical simulation curve; a) Effect of fiber winding angle.

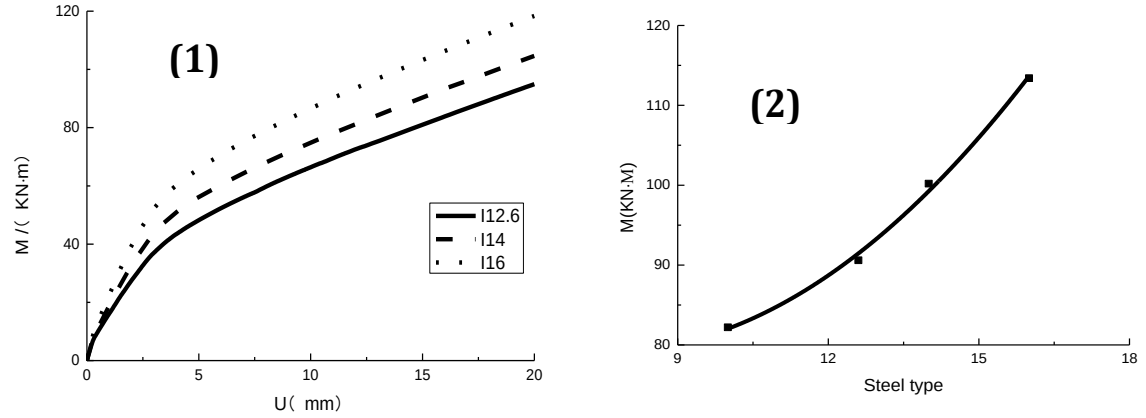

Figure 4b: Effect of steel type.

thickness of the GFRP tube, the strength grade of the concrete, the cross section and the strength of the steel. Based on the accuracy of the simulation model to design specimen, the aforementioned factors were investigated using the finite element software.

Figure 4a (1) shows the effect of fiber winding angle; it can be seen from the curve that fiber winding angle has less influence on the early loading, because the lateral expansion of the concrete and constraint effect of the GFRP tube were not obvious at this time. The deflection of the concrete was also small. As the load increased, the steel and the GFRP tube emerged the confining effect and the increasing of the component's deflection became slow. The larger the fiber winding angle, the stronger the bending resistance of the concrete became. Figure 4a (2) shows with the increasing of the fiber winding angle, bending bearing capacity have an approximate linear growth.

Figure 4a (2) indicate the effect of steel cross section. The M-μ curve showed that with the steel type change, the structure' initial stiffness enhanced along with the steel cross-sectional area's increased, elasticity segment increased and the slope of the elastic section on M-μ curve became larger, the component bending capacity greatly enhanced. Figure 4b (2) shows with the increasing of steel cross-sectional area, bending capacity have an approximation parabolic growth.

Figure 4c (1) shows the effect of concrete strength grade. Concrete is a brittle material and the concrete reached the tensile strength limit because of the load which was perpendicular to the cross section quickly at the elastic phase and the concrete tension zone quit of the job, such that the deflection was very close to the other; we can obtain a conclusion that the concrete strength grade has little effect on the bending capacity of the composite members Figure 4c (2). The bending capacity has a little growth along with the concrete strength grade increase.

The effect of steel strength

The core concrete and steel can be seen as a whole at the beginning of the force because of the bond-slip, while the

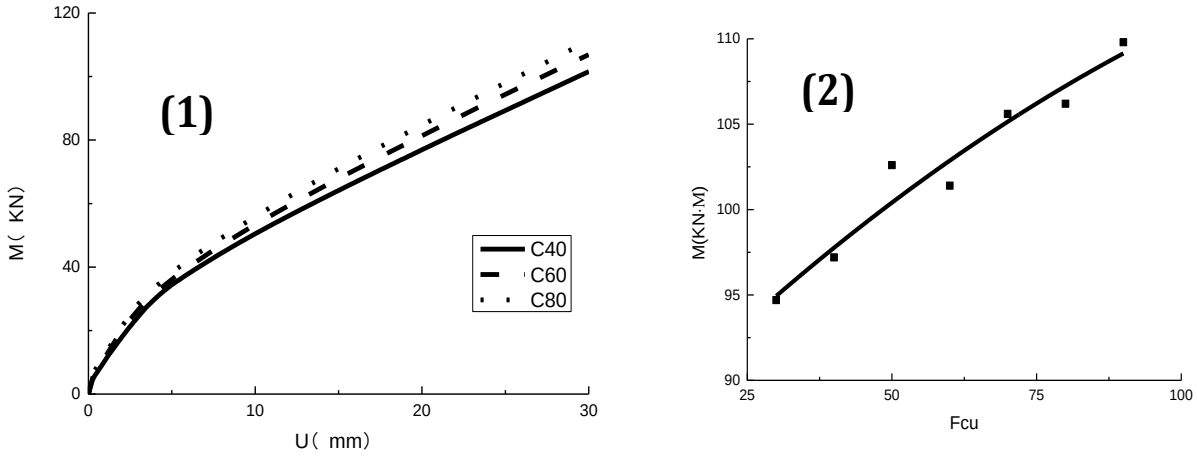

Figure 4c: Effect of concrete strength grade

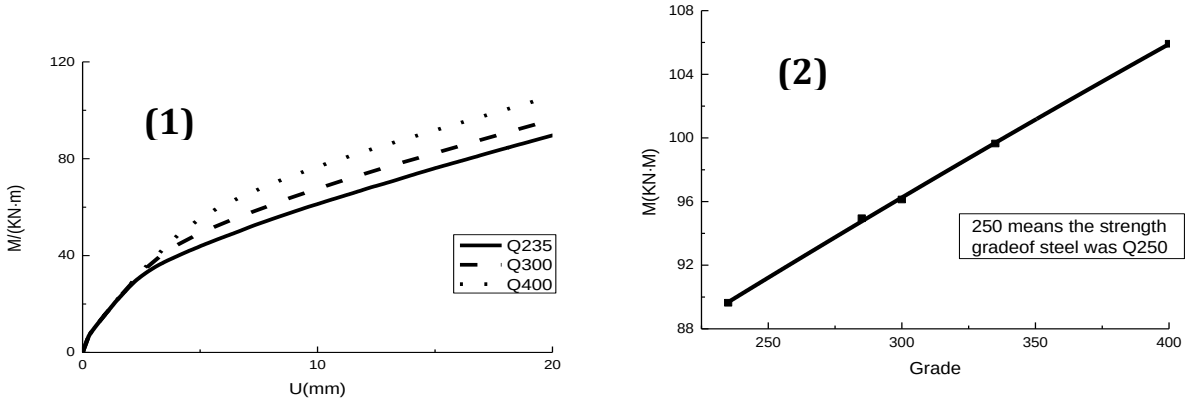

Figure 4d: Effect of steel strength.

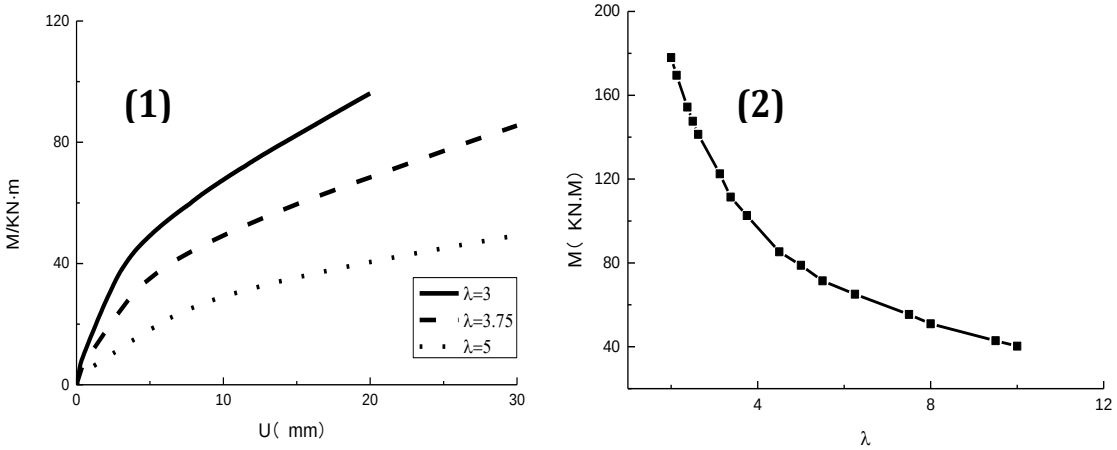

Figure 4e: Effect of cut span ratio.

high-strength steel makes the whole have a larger initial stiffness and an extended elastic section. Figure 4d (1) showed that the elastic limit of the high strength steel is larger than that of the lower strength steel and that it has high bending capacity. Figure 4d (2) showed the bending capacity has an approximate linear growth.

Figure 4e (1) showed the effect of shear span ratio. It can be seen that the effect was significant on the M-μ curve

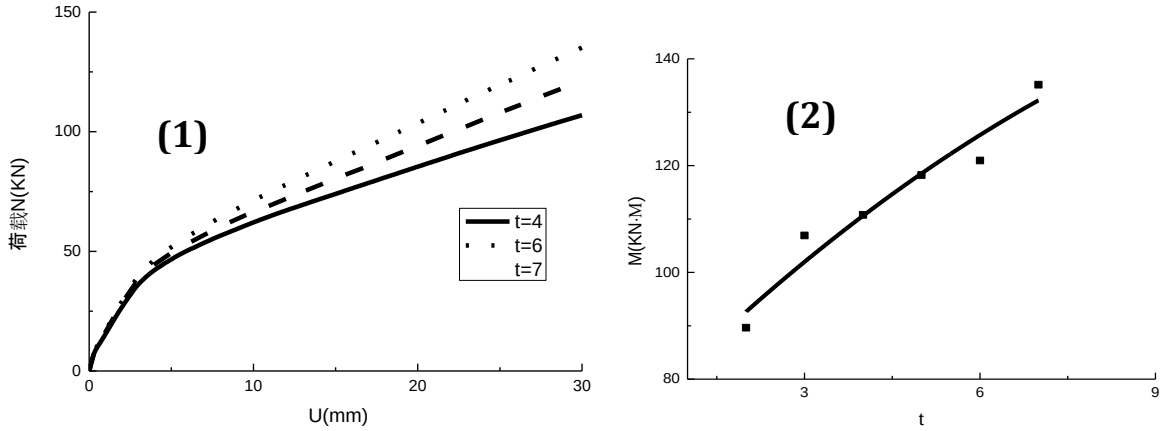

Figure 4f: Effect of GFRP wall thickness.

Table 3: Comparison of calculated and experimental values.

Specimen number	λ	θ	ρ	M_{exp}	M_{cal}	M_{cal}/M_{exp}
SW1	2.2	0.7558	0.3646	65.4	70.82	1.08
WGSC2	3	1.0077	0.3646	72.36	79.68	1.10
SW3	3.3	0.6229	0.3646	61.8	66.14	1.07

because of shear span ratio. With the increasing of the shear span ratio, the specimen is responsible for its own gravity as well as the same load. The relationship between the bending moment and the length has a quadratic function, while the increase of the bending moment causes deformation of the composite member and accelerates the decrease of the bearing capacity. Figure 4e (2) show the bearing capacity decreasing along with the shear span ratio.

Figure 4f (1) show the effect of wall thickness. It can be found from Figure 4f (1) that the composite members which had the thicker GFRP tube had the higher bending capacity because the thicker GFRP tube can be suppressed and the bearing capacity would improve. Figure 4f (2) indicate the wall thickened and the bending ability approximated linear growth.

BEARING CAPACITY FORMULA SIMPLIFIED CALCULATION

Based on the unified theory of concrete-filled steel tube (Zhong, 1994), the formula for calculating the bending capacity of the combined member was obtained in literature (Wang and Chen, 2013), but the attenuation of the bearing capacity caused by the shear ratio of the bending member was not taken into account. In this paper, based on the regression analysis of ABAQUS calculation, results and the experimental results, the bearing capacity formula was simplified as:

$$M = \varphi 0.2821r(0.89437 + 1.0001\theta + 0.9927\rho_s)A_c f_c \quad (3)$$

θ means hoop coefficient ($\theta = {f_f A_f}/{f_c A_c}$, f_f means the circumferential tensile strength of GFRP tube, A_f means the sectional area of GFRP tube), ρ_s means bone index of steel ($\rho_s = {f_s A_f}/{f_c A_c}$, f_s means the yield strength of steel, $A_s$means the steel cross-sectional area), φ means stability factor ($\varphi = 1 - \zeta\sqrt{\frac{L}{D} - 4}$, where: ζ means shear span ratio reduction factor, L means the calculation span of the beam and D means the outer diameter of the beam).

The reduction coefficient was calculated by changing the shear ratio of the specimen. It can be seen from Figure 4e that the bending moment in the mid-span decreased with the increase of the shear-span ratio, regression analysis, the calculation results and experimental results. We could obtain formula 4:

$$\begin{cases} \zeta = -0.277\lambda^2 + 1.619\lambda - 1.977 & 2 \le \lambda \le 3 \\ \zeta = 0.001\lambda^2 - 0.04\lambda + 0.502 & \lambda > 3 \end{cases} \quad (4)$$

In order to verify the applicability and accuracy of the formula of bearing capacity, the experimental data (Qin et al., 2009) were taken into equation 3 for calculation. Table 3 shows the results. The results showed that the calculated results are in agreement with the experimental results. The average score of Mcal / Mexp was 1.083 and the mean variance was 0.0125.

CONCLUSIONS

By using ABAQUS to simulate the bending properties of GFRP concrete composite members through the contrast analysis of M- μ curve, the following conclusions can be drawn:

(1) Through the comparison with the experimental M- μ curve, the numerical simulation was in good agreement with the experimental one and the accuracy of the numerical model could be verified;
(2) The influence of GFRP tube wall thickness, concrete strength grade and steel cross section and shear span ratio on the bending capacity of GFRP composite members were analyzed;
(3) Based on the numerical results and the experimental study, by using the unified theory of concrete-filled steel tube to modify the formula of bending capacity under the consideration of shear - span ratio. The formula calculated results are in good agreement with the experimental results.

REFERENCES

Cao P (2013). Mechanical behavior of steel-encased concrete filled FRP tube column under unidirectional eccentric compression[D].Shenyang Jianzhu University.

Hashin Z (1980). Failure criteria for unidirectional fiber composites. J. Appl. Mech. 47(2): 329-334

Li Y (2013). Research on mechanical properties of the reinforced concrete Filled GFRP tube beams. Northeast Petroleum University.

Nie J, Shen J (1993). Flexural strength and ductility of cross section in composite steel-concrete beams. J. Harbin Univ. Civil Eng. Architecture. pp. 235-242.

Qin G (2010). Mechanical behaviors study on GFRP tube filled with reinforced concrete members. Northeastern University.

Qin Guopeng, Wang Lianguang, Wu Di (2009). Mechanical behavior of flexural members of CFRP tube filled with steel reinforced concrete. Concrete. pp. 59-61.

Wang L, Chen B (2013). Steel reinforced concrete-filled glass fiber reinforced polymer or steel tubular structures[M].Shenyang:Liaoning Science and Technology Publishing House.

Xia Y (2011). Mechanical Behavior study on GFRP tube filled with reinforced concrete members under eccentric compression [D].Shenyang Jianzhu University.

Zhang Ni, Wang L (2014). Nonlinear analysis of flexural menbers of GFRP-concrete-steel double-skin tubular. Steel Construction, 12: 8-12.

Zhao D, Wang Q, Guan P (2003). Calculation of bearing capacity of eccentrically loaded circular steel columns filled with steel-reinforced high-strength concrete. China Harbour Eng. (255-260: 457-461.

Zhong S (1994). The unified theory of concrete filled steel tube. J. Harbin Univ. Civil Eng. Architecture. pp. 21-27.